Ocean Dynamics (2004) 54: 232–242
DOI 10.1007/s10236-003-0074-3

Jinyu Sheng · Liqun Tang

A two-way nested-grid ocean-circulation model for the Meso-American Barrier Reef System

Received: 15 January 2003 / Accepted: 24 April 2003

Abstract A two-way nested-grid ocean-circulation model is developed for the Meso-American Barrier Reef System (MBRS), using a newly developed two-way interactive nesting technique. The unique feature of this new nesting technique is its use of the semi-prognostic method (Sheng et al. 2001) to exchange information between different grids through the model momentum equations. The nested-grid model for the MBRS has a fine-resolution inner model embedded in a coarse-resolution outer model. The outer model is the western Caribbean Sea model developed by Sheng and Tang (2003), with a horizontal resolution of roughly 19 km. The inner model domain covers the northwest Caribbean Sea (NWCS) between 79°W and 89°W and between 15.5°N and 22°N, with a horizontal resolution of roughly 6 km. The nested-grid ocean model is initialized with the January mean temperature and salinity and forced by the monthly mean COADS (comprehensive ocean-atmosphere data set) wind stress and surface heat flux. The model sea-surface salinity is restored to the monthly mean climatology. The nested-grid model is integrated for 2 years and the second-year model results are presented in this paper. The model-calculated annual-mean near-surface currents over the NWCS agree reasonably well with the time-mean near-surface currents inferred by Fratantoni (2001) from trajectories of the satellite-tracked 15-m drogued drifters in the 1990s. The two-way nested model is also used to quantify the role of local wind stress, local density gradients and boundary forcings of the outer model in driving the annual-mean circulation in the region.

Responsible Editor: Phil Dyke

J. Sheng (✉) · L. Tang
Department of Oceanography,
Dalhousie University, Halifax, NS, Canada, B3H 4J1
e-mail: jinyu.sheng@dal.ca
Tel.: 902-494-2718
Fax: 902-494-2885

Keywords Two-way nesting · Numerical model · Caribbean Sea · Semiprognostic method · Ocean circulation · Process study

1 Introduction

The Meso-American Barrier Reef System (hereinafter MBRS), which extends from Isla Contoy on the north of the Yucatan Peninsula to the Bay Islands of Honduras in the western Caribbean Sea (Fig. 1), is the largest living barrier reef in the world. The MBRS serves as important breeding and feeding grounds for marine mammals, reptiles, fish and invertebrates, many of which are of commercial importance. The MBRS also contributes significantly to the protection of coastal landscapes and maintenance of coastal water quality. The unique marine ecosystems in the MBRS, however, have been significantly affected by natural and anthropogenic influences such as eutrophication of coastal waters, excessive terrestrial runoff and sedimentation from deforestation. There is an increasing demand for better understanding of the physical processes in the MBRS in order to develop more effective management plans for the sustainable use of the coastal and marine ecosystems and diverse resources in the region.

The upper ocean circulation in the MBRS is dominated by a warm and persistent throughflow known as the Caribbean Current, which enters the northwestern Caribbean Sea (NWCS) along the outer flank of Nicaragua Rise and then flows westward about 200 to 300 km off the northern coast of Honduras. The Caribbean Current veers anticyclonically to flow northward along the eastern coast of Belize and Mexico after passing the Gulf of Honduras (GOH). The current becomes known as the Yucatan Current as it flows through the western Yucatan Strait (Mooers and Maul 1998). The annual mean volume transport of the Caribbean Current through the Yucatan Strait is about 24 to 26 Sv (1 Sv = 10^6 m^3s^{-1}), according to the latest estimates of Johns et al. (2002) and Sheinbaum et al.

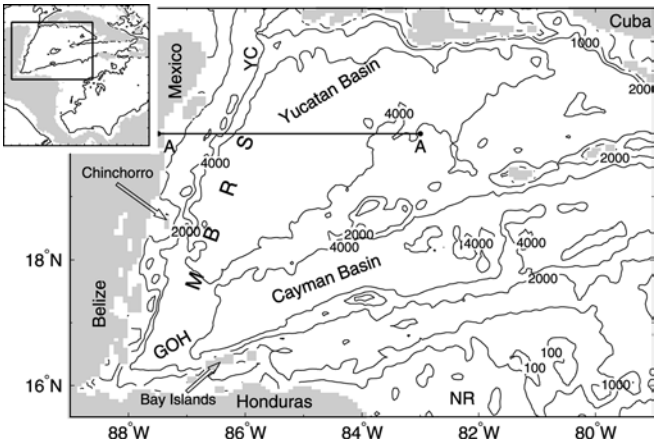

Fig. 1 Selected topographic features within the inner model domain of the nested-grid model for the northwestern Caribbean Sea. *Inset* shows the outer model domain. Abbreviations are used for the Yucatan Channel (*YC*), Meso-American Barrier Reef System (*MBRS*), Gulf of Honduras (*GOH*) and Nicaragua Rise (*NR*). *Contours* are labelled in units of metres

(2002). The physical processes in the MBRS are also significantly affected by freshwater runoff from rivers in the region. For instance, after Hurricane Mitch in 1998, the turbid waters from the rivers along the coastline of Honduras and Guatemala reached the Bay Islands in less than 1 day and reached Belize's offshore atolls within 5 days. During the same period, the estuarine plumes from Honduras extended more than 300 km towards Chinchorro Bank atoll in 3 days. Hence, a three-dimensional, baroclinic, eddy-resolving ocean-circulation model is needed to improve current understanding of the physical processes at work in the MBRS and eventually predict ocean circulation and dispersion at various temporal and spatial scales in the region.

The main objectives of this paper are (1) to present a two-way nested-grid primitive equation ocean-circulation model of the NWCS; and (2) to use this nested-grid model to study the general circulation and temperature/salinity distributions in the region. In this paper we consider the fixed-space nesting in the horizontal direction with a fine-grid inner model embedded in a coarse-grid outer model. We also follow others (e.g. Kurihara et al. 1979; Oey and Chen 1992; Ginis et al. 1998) and interpolate the outer model results onto the fine grid to drive the inner model and interpolate the inner model results back onto the coarse grid to drive the outer model. The newly developed two-way interactive nesting technique suggested by J. Sheng et al. (2003, personal communication) is used in this study. The unique feature of this new nesting technique is its use of the semiprognostic method to exchange information between the outer and inner models over the common region where the two model domains overlap. The semiprognostic method was developed originally to correct a primitive-equation ocean-circulation model for systematic error. This method replaces the density term in the hydrostatic equation with a linear combination of model-computed and climatological density (Sheng et al. 2001). This procedure corresponds to adding a forcing term to the momentum equations through the computation of the horizontal pressure gradient terms. The semiprognostic method is adiabatic, with the temperature and salinity equations unconstrained and fully prognostic.

The arrangement of this paper is as follows. Section 2 briefly reviews the ocean-circulation model and the semiprognostic method. Section 3 discusses the new two-way interactive nesting technique based on the semiprognostic method. Section 4 presents the two-way nested model results and limited sensitivity and process studies. Section 5 is a summary and conclusion.

2 The ocean-circulation model and semiprognostic method

The ocean-circulation model used in this study is the three-dimensional primitive-equation z-level ocean model known as CANDIE (Canadian version of DieCAST, Sheng et al. 1998). CANDIE is an outgrowth of the DieCAST model developed by Dietrich et al. (1987) and has successfully been applied to various modelling problems on the shelf, including wind-driven circulation over an idealized coastal canyon (Sheng et al. 1998), non-linear dynamics of a density-driven coastal current (Sheng 2001), tidal circulation in the Gulf of St. Lawrence (Lu et al. 2001) and wind-driven circulation over a stratified coastal embayment (Davidson et al. 2001). Most recently, CANDIE has been applied to the northwestern Atlantic Ocean from northern Labrador to Maine by Sheng et al. (2001) and the western Caribbean Sea by Sheng and Tang (2003). Discussions on the governing equations and sub-gridscale mixing parameterizations used in CANDIE are found in the Appendix.

It is important to note that the model governing equations presented in the Appendix are conventional except for the hydrostatic equation that was modified as (see also Eq. A4 in the Appendix):

$$\frac{\partial p}{\partial z} = -\hat{\rho} g \tag{1}$$

with

$$\hat{\rho} = \alpha \rho_m + (1-\alpha)\rho_c \ , \tag{2}$$

where g is the gravitational acceleration, $\partial p/\partial z$ on the LHS of Eq. (1) is the vertical pressure gradient, and the RHS of Eq. (2) represents the main feature of the semiprognostic method developed by Sheng et al. (2001). Here, the density term in the hydrostatic equation $\hat{\rho}$ is expressed as a linear combination of model-calculated density ρ_m and climatological density ρ_c, where α is the linear combination coefficient with a value between 0 and 1. It is readily seen that the ocean-circulation model is purely prognostic if $\alpha = 1$ and purely diagnostic if $\alpha = 0$.

As discussed in Sheng et al. (2001), the semiprognostic method is designed to adjust the momentum

equations of an ocean-circulation model to correct for the model errors associated with the physical processes that are not correctly represented by the model equations, leaving the temperature and salinity equations unconstrained and fully prognostic. To demonstrate this, we follow Sheng et al. (2001) and separate the pressure variable p into two parts:

$$p = p^* + \tilde{p} \ , \tag{3}$$

where

$$\frac{\partial p^*}{\partial z} = -\rho_m g \tag{4}$$

$$\frac{\partial \tilde{p}}{\partial z} = -(1-\alpha)(\rho_c - \rho_m)g \ . \tag{5}$$

Writing the horizontal momentum equations in terms of p^* and $\tilde{p}$ we obtain:

$$\frac{\partial u}{\partial t} = -\frac{1}{\rho_o R\cos\phi}\frac{\partial p^*}{\partial \lambda} - \frac{1}{\rho_o R\cos\phi}\frac{\partial \tilde{p}}{\partial \lambda} + \text{others} \ , \tag{6}$$

$$\frac{\partial v}{\partial t} = -\frac{1}{\rho_o R}\frac{\partial p^*}{\partial \phi} - \frac{1}{\rho_o R}\frac{\partial \tilde{p}}{\partial \phi} + \text{others} \ . \tag{7}$$

It can be seen that p^* corresponds to the traditional pressure variable carried by the model, since p^* satisfies the conventional hydrostatic equation and surface boundary condition. On the other hand, the terms involving $\tilde{p}$ in Eqs. (6) and (7) appear as additional forcing terms in the model momentum equations. It is these forcing terms that are responsible for modifying the model-computed velocities, that, in turn, modify the temperature and salinity equations through the advection terms in Eqs. (A7) and (A8) in the Appendix. Physically, therefore, the forcing terms associated with $\tilde{p}$ can be thought of as representing unresolved processes.

The two-way nested-grid ocean-circulation model developed for the MBRS has a fine-grid inner model and a coarse-grid outer model and uses the ETOPO5 topography, a gridded elevation/bottom topography for the world compiled by the US National Geophysical Data Center, National Oceanic and Atmospheric Administration. Both the inner and outer models have 31 unevenly spaced z levels with the centres of each level located at 5, 16, 29, 44, 61, 80, 102, 128, 157, 191, 229, 273, 324, 383, 450, 527, 615, 717, 833, 967, 1121, 1297, 1500, 1733, 2000, 2307, 2659, 3063, 3528, 4061 and 4673 m, respectively.

The inner model domain covers the NWCS between 79°W and 89°W and between 15.5°N and 22°N with a horizontal resolution of about 6 km. The outer model is the western Caribbean Sea (WCS) model developed recently by Sheng and Tang (2003), which covers the area between 72°W and 90°W and between 8°N and 24°N (Fig. 1) with a horizontal resolution of about 19 km. The model time steps are 16 min for the outer model and 5 min for the inner model. Both the outer and inner models also use the semiprognostic method with $\alpha = 0.5$ to reduce the model drift in multiyear simulations.

At the lateral closed boundaries of the inner and outer models, the normal flow, tangential stress of the currents and horizontal fluxes of temperature and salinity are set to zero (free-slip conditions). Along the open boundaries of the inner and outer models, the normal flow, temperature and salinity fields are calculated using the method similar to the adaptive open-boundary conditions suggested by Marchesiello et al. (2001). It first uses an explicit Orlanski radiation condition (Orlanski 1976) to determine whether the open boundary is passive (outward propagation) or active (inward propagation). If the open boundary is passive, the model prognostic variables are radiated outward to allow any perturbation generated inside the model domain to propagate outward as freely as possible. If the open boundary is active, the outer model prognostic variables at the open boundary are restored to the monthly mean climatologies with the time scale of 15 days, and the inner model prognostic variables at the open boundary are restored to the outer model results with the time scale of 5 h. In addition, the depth-mean normal flow across the outer model open boundaries is set to be the monthly mean results produced by a (1/3)° Atlantic model known as FLAME (family of linked Atlantic model experiments, Dengg et al. 1999).

3 A new two-way interactive nesting technique

The main purpose of a nested-grid ocean-circulation model is to increase grid resolution in a subregion (or more) of the whole model domain to resolve some fine-scale effect without having a computational expense of high resolution over the whole domain (Fox and Maskell 1995). A simple nested model consists of one coarse-grid model for the whole domain and one fine-grid model for the subregion. The two-way interaction between the two models can be achieved in many ways. A common nesting technique is to transfer information between the two models at a narrow zone (dynamic interface) near the grid interface frequently (e.g. Kurihara et al. 1979). The coarse-grid model variables, such as currents, temperature, salinity and associated fluxes, at the dynamic interface are interpolated onto the fine grid to force the fine-grid model. The fine-grid model variables are interpolated back onto the coarse grid to drive the coarse-grid model. The dynamic interface can then be considered as an internal boundary of the coarse-grid model, and the coarse-grid integration is not necessary over the subregion covered by the fine-grid domain. An alternative nesting technique is to embed the fine-grid inner model inside the coarse-grid outer model and use the inner model variables to replace the outer model variables over the subregion where the two grids overlap (e.g. Oey and Chen 1992).

In this study we follow Oey and Chen (1992) and consider only the fixed-space nesting in the horizontal

direction with a fine-grid inner model embedded inside a coarse-grid outer model. The two-way interactive nesting technique (J. Sheng et al. 2003, personal communication) used in this study is based on the semiprognostic method, in which the inner model is affected by the outer model in two ways. First, the outer model variables, such as currents, temperature and salinity, at the dynamic interface are interpolated onto the fine grid to provide the boundary conditions for the inner model (Sect. 2). Second, the outer model density $\hat{\rho}_{\text{outer}}$ over the common subregion where the two model grids overlap is interpolated onto the fine grid to adjust the momentum equations of the inner model. The adjustment is accomplished by expressing $\hat{\rho}$ in the hydrostatic equation of the inner model as:

$$\hat{\rho} = \alpha[\beta_i \rho_{\text{inner}} + (1-\beta_i)\tilde{\rho}_{\text{outer}}] + (1-\alpha)\rho_c \quad \text{(for the inner model)} \ , \tag{8}$$

where ρ_{inner} is the inner model density calculated from the inner model temperature and salinity, $\tilde{\rho}_{\text{outer}}$ is the outer model density interpolated onto the fine grid, ρ_c again is the climatological density, and β_i is the linear combination coefficient with a value between 0 and 1.

In return, the inner model density ρ_{inner} is interpolated back onto the coarse grid to adjust the momentum equations of the outer model over the common subregion. The adjustment is accomplished by expressing $\hat{\rho}$ in the hydrostatic equation of the outer model as

$$\hat{\rho} = \alpha[\beta_{\text{o}} \rho_{\text{outer}} + (1-\beta_o)\tilde{\rho}_{\text{inner}}] + (1-\alpha)\rho_c \ \text{(for the outer model)} \ , \tag{9}$$

where ρ_{outer} is the outer model density calculated from the outer model temperature and salinity, $\tilde{\rho}_{\text{inner}}$ is the inner model density interpolated onto the coarse grid, and β_{o} is the linear combination coefficient with a value between 0 and 1.

The above two-way interaction can be made frequently at the outer model time interval. Since the present nesting system is driven by the monthly forcings, we set the interaction rate of the two models to be once per day. In this study, we set α, β_i and β_{o} to 0.5 without conducting any sensitivity studies. It should be noted that a conventional one-way nested-grid model can be constructed by setting both β_i and β_{o} to unity. More discussion about this conventional one-way nested model is given in Section 4.2.

It is important to note that the newly developed two-way nesting technique used in this study exchanges only the density fields between the inner and outer models based on the semiprognostic method. The new nesting technique does not exchange the model-calculated currents, temperature and salinity fields directly between the two models, except that the outer model currents, temperature and salinity are used to provide the open-boundary conditions of the inner model.

4 Model results

4.1 Two-way nested model results

The two-way nested ocean model is initialized with the January mean climatological temperature and salinity and forced by the monthly mean COADS (comprehensive ocean-atmosphere data set, da Silva et al. 1994) surface wind stress and heat flux. The net heat flux through the sea surface (Q_{net}) is expressed as (Barnier et al. 1995):

$$Q_{\text{net}} = Q_{\text{net}}^{\text{clim}} + \beta\left(SST^{\text{clim}} - SST^{\text{model}}\right) \ , \tag{10}$$

where $Q_{\text{net}}^{\text{clim}}$ is the monthly mean COADS net heat flux interpolated onto the model grid and taken from da Silva et al. (1994), and β is the coupling coefficient defined as $\Delta z_1 \rho_{\text{o}} c_p / \tau_Q$, where Δz_1 is the thickness of the top z level, c_p is the specific heat, and τ_Q is the restoring time scale which is set to 15 days. The implied value of β is about 35 W m^{-2} K^{-1}, which is comparable to values calculated from observations (e.g. Haney 1971). We also restore the model salinity in the top 10 m to the monthly mean climatology with a time scale of 15 days.

We integrate the two-way nested-grid model for 2 years (referred to as the control run) and calculate the annual mean volume transport streamfunction (Fig. 2) from the second-year model simulation. The annual mean streamfunction produced by the two-way nested outer model has large-scale spatial features highly comparable to that produced by the single-domain WCS model (see Sheng and Tang 2003; and also see the one-way nested outer model results in Fig. 2b). The depth-integrated circulation produced by the two-way nested outer model is characterized by a strong barotropic circulation associated with the Caribbean Current. The depth-integrated flow runs westward about 200–300 km off the northern coast of South America and then northward along the eastern coast of Central America. There is a barotropic recirculation associated with the Panama–Colombia Gyre over the southwest Caribbean. The annual-mean volume transport is about 19 Sv for the Caribbean Current over the eastern Colombian Basin, 7 Sv for the westward flow through the Windward Passage and 26 Sv for the northward flow through the Yucatan Strait. All of the above mean transport values are consistent with the current knowledge of the mean transport in the region (Murphy et al. 1999; Johns et al. 2002).

The large-scale features of the annual-mean transport streamfunction produced by the two-way nested inner model are highly coherent with those produced by the two-way nested outer model over the NWCS, with some differences in small-scale features (Fig. 2a). There is about 26 Sv of the inflow that enters the NWCS through the southern and eastern inner model open boundaries. Among this total inflow, about 16 Sv comes from the Colombian Basin through the transect between Honduras and Jamaica. The rest comes from the transect between Jamaica and Cuba.

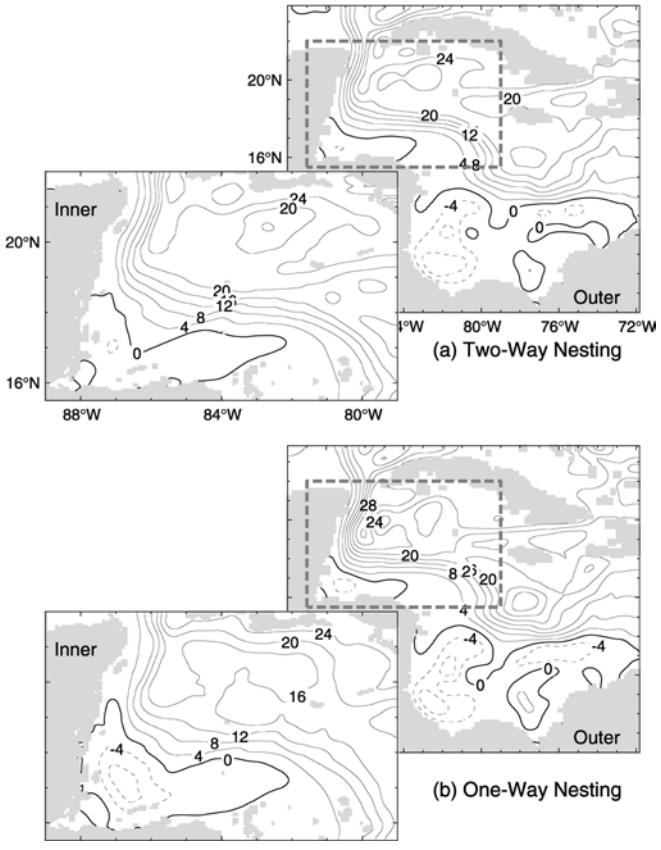

Fig. 2a, b Annual-mean volume transport streamfunctions calculated from the second-year model results using **a** the two-way nesting technique and **b** the conventional one-way nesting technique. *Contours* are labelled in units of Sv ($= 10^6\ \mathrm{m^3\ s^{-1}}$) and *contour intervals* are 4 Sv

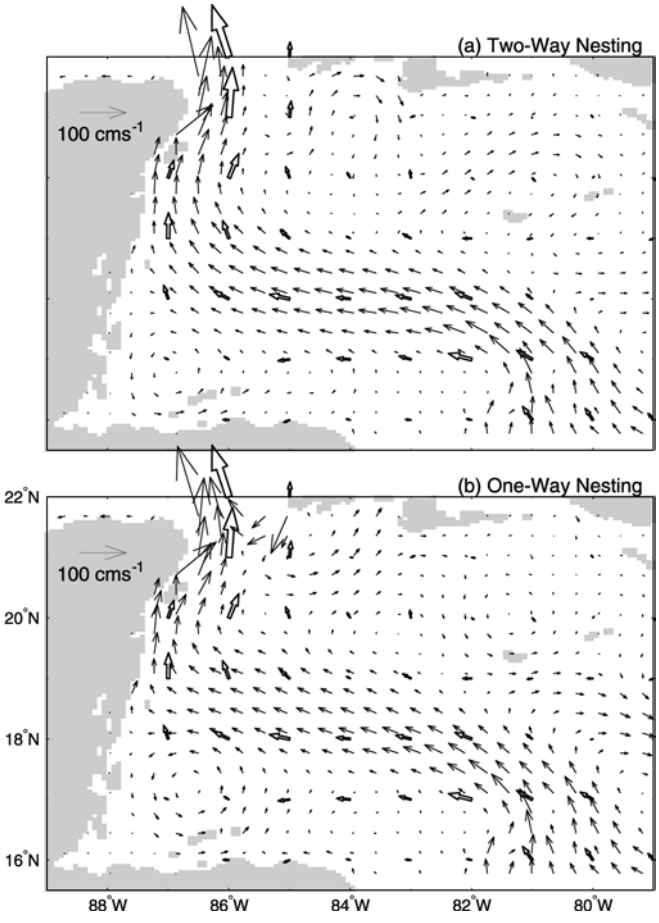

Fig. 3a, b Comparison of model-calculated (*solid arrows*) and observed (*open arrows*) near-surface currents over the northwestern Caribbean. The model-calculated currents are the annual mean near-surface currents at 16 m computed from the second-year results produced by the inner model using **a** the two-way nesting technique and **b** the conventional one-way nesting technique. Model velocity vectors are plotted at every sixth model grid point. The observed currents are the gridded decadal-mean near-surface currents during the 1990s inferred from trajectories of 15-m drogued satellite-tracked drifters by Fratantoni (2001) on a 1° grid

We compute the annual-mean near-surface currents at 16 m from the second-year inner model simulation and compare them with the decadal mean near-surface currents inferred by Fratantoni (2001) from trajectories of the satellite-tracked 15-m drogued drifters made during the 1990s in Fig. 3a. The two-way nested inner model results reproduce reasonably well the main pathway of the observed Caribbean Current in the upper ocean of the NWCS. The inner model results exhibit that the Caribbean Current flows first northwestward along the northeastern flank of Nicaragua Rise and then westward about 200–400 km off the northern coast of Honduras. The Current turns northward over the Gulf of Honduras (GOH) and flows northward along the eastern coast of Belize and Mexico. The inner model also generates a strong northward flow over the western portion of the Yucatan Strait, with a maximum near-surface flow greater than 230 cm $\mathrm{s^{-1}}$. The near-surface currents over the eastern Yucatan Basin are relatively weak.

To measure the misfit between the observations and the model-computed near-surface currents in the NWCS shown in Fig. 3a, we use a value of γ^2 defined as:

$$\gamma^2 = \frac{\sum_k^N \left[(u_k^{\mathrm{o}} - u_k^{\mathrm{s}})^2 + (v_k^{\mathrm{o}} - v_k^{\mathrm{s}})^2 \right]}{\sum_k^N \left[(u_k^{\mathrm{o}})^2 + (v_k^{\mathrm{o}})^2 \right]}\ , \qquad (11)$$

where $(u_k^{\mathrm{o}}, v_k^{\mathrm{o}})$ are the horizontal components of the observed near-surface currents at the kth location estimated by Fratantoni (2001), $(u_k^{\mathrm{s}}, v_k^{\mathrm{s}})$ are the horizontal components of the simulated near-surface currents produced by the inner model at the kth location as the observations, and N is the total number of locations where observations were made. Clearly, the smaller γ^2, the better the model results fit the observations. For the two-way nested inner model results shown in Fig. 4a, the value of γ^2 is 0.4.

4.2 Sensitivity study: one-way and two-way nesting

To demonstrate the advantage of the newly developed two-way nesting approach in resolving fine-scale

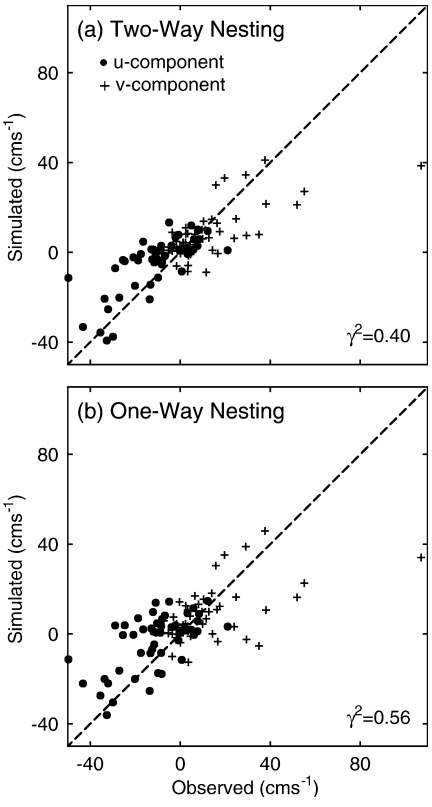

Fig. 4a, b Scatterplots of observed and model-computed time-mean near-surface currents in the northwest Caribbean Sea. The observed currents are the decadal-mean near-surface currents during the 1990s inferred from trajectories of 15-m drogued satellite-tracked drifters by Fratantoni (2001). The model-computed currents are those at the same locations as the observations interpolated from the second-year model simulations at 16 m using **a** the two-way nesting technique and **b** the conventional one-way nesting technique

circulation features in the NWCS, we compare the model results produced by the two-way and one-way nesting techniques. A conventional one-way nesting technique is the one using the coarse-grid outer model results such as currents, temperature and salinity, to provide the boundary conditions for the fine-grid inner model without any feedback from the inner model to the outer model. The conventional one-way nested model, as mentioned in Section 3, can be constructed by setting β_i and β_o to unity. The density term in the model hydrostatic equation can be expressed as:

$$\hat{\rho} = \alpha\rho_{\text{inner}} + (1-\alpha)\rho_c \quad \text{(for the inner model)} \ , \qquad (12)$$

$$\hat{\rho} = \alpha\rho_{\text{outer}} + (1-\alpha)\rho_c \quad \text{(for theouter model)} \ , \qquad (13)$$

where ρ_{inner} and ρ_{outer} are the inner model density and outer model density, respectively, and ρ_c again is the climatological density. It is interesting to note that an alternative one-way nested model can be constructed by setting β_o to unity but setting β_i to less than 1. In this non-conventional one-way nesting system the outer model results are used not only to provide boundary conditions for the inner model, but also to adjust the momentum equations of the inner model based on the semiprognostic method (we call this the semiprognostic one-way nesting technique). Discussion of this semiprognostic one-way nesting technique is presented in J. Sheng et al. (2003, personal communication). We consider only the conventional one-way nesting technique in this paper.

We drive the conventional one-way nested-grid model with the same external forcings as in the control run. We integrate the conventional one-way nesting system for 2 years and calculate the annual-mean volume transport streamfunction from the second-year simulation (Fig. 2b). The overall features of the annual mean streamfunction produced by the one-way nested outer model are in good agreement with those produced by the two-way nested outer model (Fig. 2a). Some small differences occur, however, between the annual-mean streamfunctions produced by the inner models of the two nesting systems. In comparison with the two-way nested inner model results, the conventional one-way nested inner model generates a relatively stronger cyclonic recirculation over the GOH and adjacent areas. Some small differences also occur in the annual-mean streamfunctions produced by the outer models of the two nesting systems. These differences can be explained by the feedback from the inner model to the outer model in the two-way nesting system (Fig. 2a and b).

The annual-mean near-surface currents at 16 m produced by the conventional one-way nested inner model have large-scale spatial features very similar to those produced by the two-way nested inner model (Fig. 3a and b). There are, however, considerable differences in small-scale features produced by the inner models of the two nesting systems over the GOH and the eastern Yucatan Basin. Furthermore, the simulated Caribbean Current produced by the conventional one-way nested inner model is relatively weaker and broader than that produced by the two-way nested inner model. There are also considerable differences in the direction of the simulated Caribbean Current over the western Cayman Basin produced by the two inner models. Figure 3 also demonstrates that the conventional one-way nested inner model results agree with the decadal mean near-surface currents inferred by Fratantoni (2001) less well than the two-way nested inner model results. The γ^2 value for the conventional one-way nested inner model results is 0.56 (Fig. 4b), which is about 40% larger than the γ^2 value of the two-way nested inner model results. Therefore, the two-way nesting technique performs better than the conventional one-way nesting technique in simulating the annual mean near-surface circulation in the NWCS.

To demonstrate the advantage of the newly developed two-way nesting technique in resolving fine-scale features at shorter time scales, we next discuss the monthly mean circulation computed from the second-year model results produced by the two-way and the conventional one-way nesting techniques. The January mean near-surface currents at 16 m over the NWCS produced by the two-way nested inner and outer models

are highly coherent (Fig. 5a), with small-scale circulation features resolved better by the inner model. By contrast, the one-way nested inner model results differ significantly from the one-way outer model results, indicating that the conventional one-way nested inner model drifts away from the outer model, which is the common problem of the conventional one-way nesting technique. There are also some differences in the outer model results of the two-way and one-way nesting systems (Fig. 5). These differences are again associated with the feedback from the inner model to the outer model in the two-way nesting system.

The instantaneous model results shown in Fig. 6 demonstrate clearly that the newly developed two-way nesting technique performs better than the conventional one-way nesting technique in resolving fine-scale circulation features in the NWCS. The near-surface currents and temperature at 16 m at day 120 produced by the two-way nested model are characterized by northwestward advection of relatively warm waters from the Colombian Basin to the NWCS, with several small-scale recirculations on both sides of the Caribbean Current. The large-scale circulation features of the instantaneous near-surface circulation and temperature produced by the two-way nested inner model are highly coherent to those produced by the the two-way nested outer model, with several small-scale features better resolved by the fine-resolution inner model, as expected. In comparison, the conventional one-way nesting technique produces significantly large differences between the inner and outer model results. In fact, the conventional one-way nested inner model generates several large-scale gyres rather than the warm and persistent Caribbean Current over the NWCS, which diverges significantly from the outer model results.

4.3 Process study: the role of local wind, boundary forcing and local density gradients

We conduct three additional numerical experiments to examine the role of local wind stress, boundary forcing and local density gradients in driving general circulation in the NWCS. The two-way nested-grid model is used with the same model parameters as in the control run. The model external forcings are also the same as those in the control run, except that (1) the local wind stress is set to zero in the first experiment (the no-local-wind case); (2) depth mean flows across the outer model open

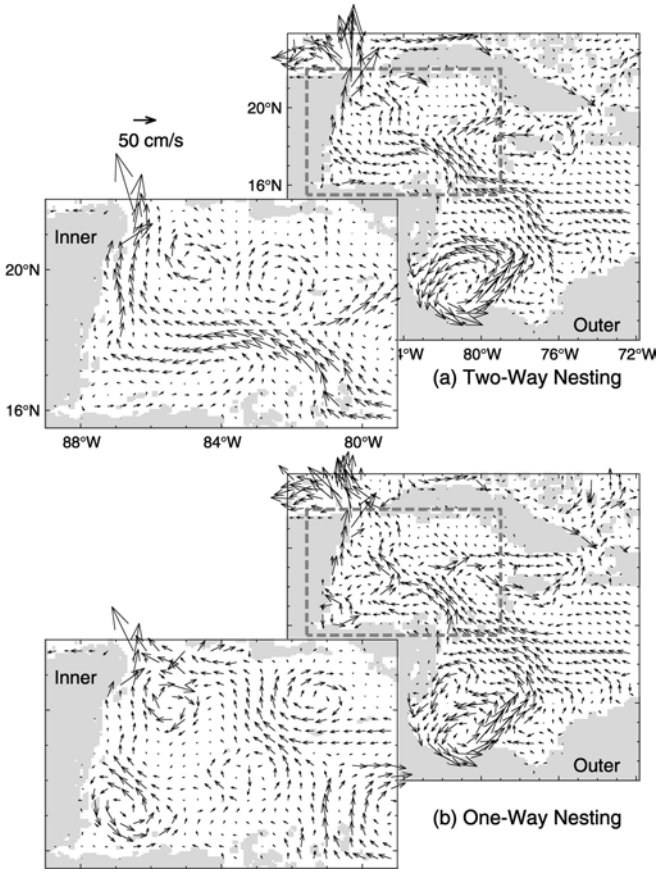

Fig. 5a, b January-mean near-surface currents at 16 m calculated from the second-year simulations using **a** the two-way nesting technique and **b** the conventional one-way nesting technique. Velocity vectors are plotted at every sixth model grid point

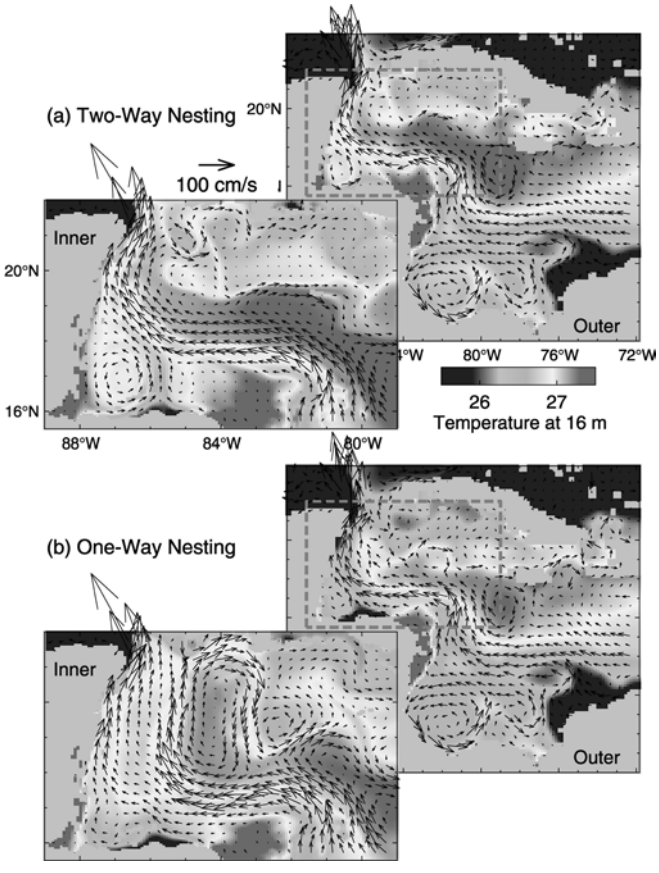

Fig. 6a, b Instantaneous temperature (-grey image) and currents (*arrows*) at 16 m at day 120 produced by **a** the two-way nesting technique and **b** the conventional one-way nesting technique. Velocity vectors are plotted at every sixth model grid point

boundaries are set to zero in the second experiment (the no-boundary-forcing case); and (3) temperature and salinity at each model grid point are set to constant values of 15 °C and 36 ppt, respectively, in the third experiment (the uniform-density case). We integrate these three cases individually for 2 years and calculate the annual-mean transport streamfunctions (Fig. 7) from the second-year model simulations.

The annual-mean transport streamfunction in the no-local-wind case has a general spatial distribution which is very similar to that in the control run, with some differences in small-scale features (Fig. 7a and b). By contrast, the annual-mean transport streamfunction in the no-boundary-forcing case is significantly different from that in the control run (Fig. 7a and c). Figure 7d shows that, except for the values over the areas adjacent to the model open boundaries where the results are affected by the boundary conditions, the mean transport streamfunction in the uniform density case follows the bottom topography much more closely than that in the control run. Figure 8 compares the northward components of vertically integrated currents in the upper ocean of less than 90 m (V_{upp}) and lower ocean of deeper than 90 m (V_{low}) along transect A–A at 20°N off the east coast of Mexico (Fig. 1) in the four cases. The zonal distributions of V_{upp} and V_{low} in the no local wind case are comparable to those in the control run. The upper ocean values of V_{upp} in the no-local-wind case are only about 10% smaller than those in the control run within the range of 150 km from the east coast of Mexico. In the cases of no-boundary-forcing and uniform density, the zonal distributions of V_{upp} in the upper ocean are much smaller than those in the control run. The zonal distributions of V_{low} in the lower ocean in these two cases are, however, remarkably distinct from those in the control run.

We also compare the annual-mean near-surface currents in the four cases with the decadal mean near-surface currents inferred by Fratantoni (2001) in Figs. 9 and 10. The model results in the no-local-wind case underestimates the observed near-surface currents

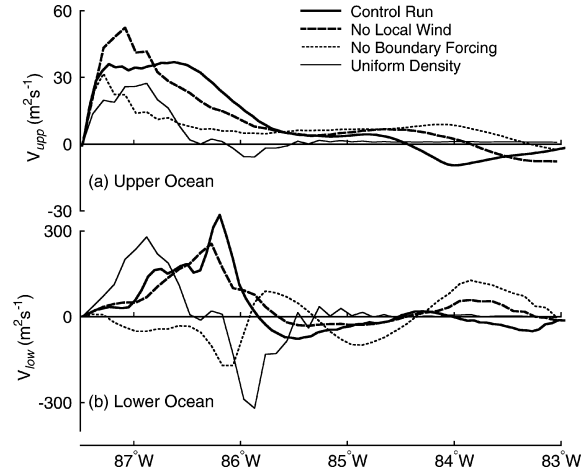

Fig. 8 The northward component of the depth-integrated flow in the upper ocean (less than 90 m) and lower ocean (deeper than 90 m) across transect at 20°N off the east coast of Mexico

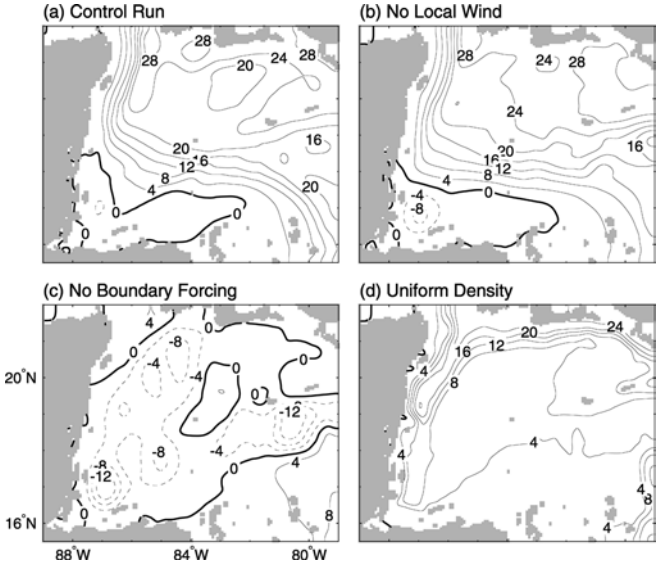

Fig. 7a–d Annual-mean transport streamfunctions calculated by the two-way nested model in the four cases. The model external forcings are same as **a** in the control run except that **b** the wind stress is set to zero (the no-local-wind case); **c** depth mean flows across the outer model open boundaries are set to zero (the no-boundary-forcing case); and **d** temperature and salinity at each model grid point are set to constant values of 15 °C and 36 ppt, respectively (the uniform-density case). *Contours* are labelled in units of Sv (= $10^6\,m^3\,s^{-1}$) and *contour intervals* are 4 Sv

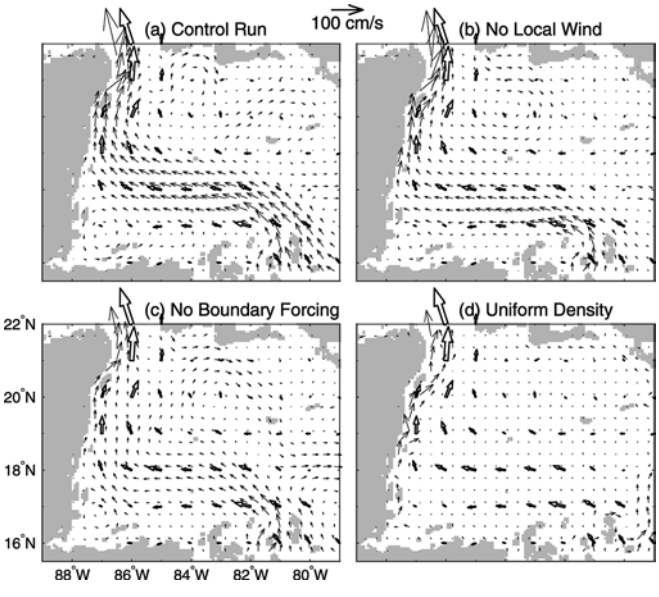

Fig. 9 Annual-mean near-surface currents (*solid arrows*) at 16 m calculated from the second-year simulations in the four cases. Model velocity vectors are plotted at every sixth model grid point. The observed currents (*open arrows*) are the gridded decadal-mean near-surface currents during the 1990s inferred from trajectories of 15-m drogued satellite-tracked drifters by Fratantoni (2001) on a 1° grid. Otherwise, as Fig. 7

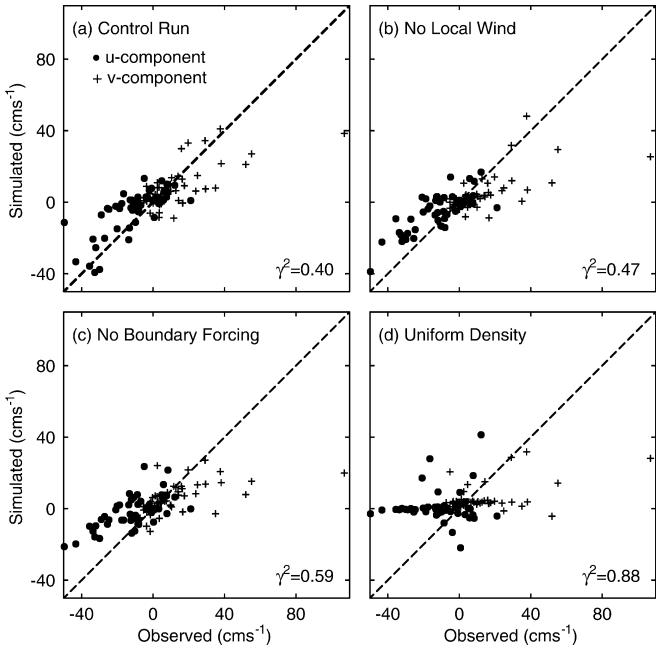

Fig. 10 Scatterplots of observed and model-calculated time-mean near-surface currents in the four cases. The observed currents are the decadal-mean near-surface currents during the 1990s inferred from trajectories of 15-m drogued satellite-tracked drifters by Fratantoni (2001). The model-computed currents are those at the same locations as the observations interpolated from the second-year model simulations in the four cases

(Fig. 9b). The γ^2 in the no-local-wind case is 0.47, which is about 20% larger than that in the control run. The model results in the no-boundary-forcing and uniform density cases fail to reproduce the main features of the observed near-surface currents in the NWCS (Fig. 9c and d). The γ^2 values in these two cases are 0.59 and 0.88 (Fig. 10c and d), which are, respectively, about 50 and 120% larger than in the control run. It can be concluded, therefore, that baroclinicity and boundary forcing of the outer model play a very important role in driving the annual-mean circulation in the NWCS. The local wind forcing also plays an important role in driving the near-surface circulation, but a minor role in driving the volume transport streamfunction in the region.

5 Summary and conclusion

We developed a two-way nested-grid ocean circulation model for the Meso-American Barrier Reef System. We followed Oey and Chen (1992) in this study and considered only the fixed-space nesting with a fine-grid inner model embedded inside a coarse grid outer model. The outer model is the western Caribbean Sea model developed recently by Sheng and Tang (2003), with a horizontal resolution of roughly 19 km. The inner model domain covers the northwest Caribbean Sea between 79°W and 89°W and between 15.5°N and 22°N, with a horizontal resolution of roughly 6 km. We forced the nested model with the climatological monthly mean forcing including local wind stress, surface heat and freshwater fluxes. We also used the monthly mean model results produced by the FLAME to specify the boundary flows of the outer model. We used the two-way nested-grid model to simulate the annual-mean circulation in the NWCS, and compared the model results with the decadal mean near-surface currents determined by Fratantoni (2001) from the trajectories of the near-surface drifters made in the 1990s. The model results reproduce many well-known circulations in the NWCS. We also used the two-way nested-grid model to examine the role of local wind stress, boundary forcing of the outer model and local density gradients in driving the general circulation in the NWCS. We demonstrated that the boundary forcing of the outer model and baroclinicity play a very important role in driving the annual mean circulation in the NWCS. The local wind forcing also plays an important role in driving the near-surface circulation. The local wind forcing, however, plays a minor role in driving the depth-integrated flow in the region.

We used the newly developed two-way interactive nesting technique suggested by J. Sheng et al. (2003, personal communication) in the development of the two-way nested model for the MBRS. This new nesting technique is based on the semiprognostic method, which was originally developed to correct for the model systematic errors (Sheng et al. 2001). In this study we followed J. Sheng et al. (2003, personal communication) and used the semiprognostic method to exchange the model density fields between the inner and outer models through the horizontal pressure gradient terms in the momentum equations. Except that the outer model currents, temperature and salinity fields are used to provide open-boundary conditions of the inner model, the newly developed two-way interactive nesting technique does not exchange directly the model currents, temperature and salinity fields between the inner and outer models, which is advantageous over other existing techniques. In addition, the new nesting technique is computationally stable and relatively easy to implement.

Acknowledgements We wish to thank Richard Greatbatch, Chris Mooers, Leo Oey, Alan Davies, Jiuxing Xing, Bruce Hatcher and Barry Ruddick for their useful suggestions and comments. We are also grateful to Carsten Eden for making his model results available to us. This project is part of the ECONAR (Ecological Connections Among Reefs) supported by the Collaborative Research Opportunity Program of the Natural Sciences and Engineering Research Council of Canada (NSERC). J.S. is also supported by NSERC, MARTEC (a Halifax-based company), and the Meteorological Service of Canada (MSC) through the NSERC/MARTEC/MSC Industrial Research Chair in Regional Ocean Modelling and Prediction.

Appendix: Basic equations of the ocean circulation model

The three-dimensional primitive-equation ocean-circulation model known as CANDIE (http://www.phys.ocean.dal.ca/programs/CANDIE, or see Sheng et al.

1998, 2001) is used in this study. The governing equations of the model can be written in spherical coordinates as:

$$\frac{\partial u}{\partial t} + \mathcal{L}u - \left(f + \frac{u\tan\phi}{R}\right)v = -\frac{1}{\rho_o R\cos\phi}\frac{\partial p}{\partial \lambda} + \mathcal{D}_m u + \frac{\partial}{\partial z}\left(K_m \frac{\partial u}{\partial z}\right) \ , \quad \text{(A1)}$$

$$\frac{\partial v}{\partial t} + \mathcal{L}v + \left(f + \frac{u\tan\phi}{R}\right)u = -\frac{1}{\rho_o R}\frac{\partial p}{\partial \phi} + \mathcal{D}_m v + \frac{\partial}{\partial z}\left(K_m \frac{\partial v}{\partial z}\right) \ , \quad \text{(A2)}$$

$$\frac{1}{R\cos\phi}\left(\frac{\partial u}{\partial \lambda} + \frac{\partial (v\cos\phi)}{\partial \phi}\right) + \frac{\partial w}{\partial z} = 0 \ , \quad \text{(A3)}$$

$$\frac{\partial p}{\partial z} = -[\alpha\rho_m + (1-\alpha)\rho_c]g \ , \quad \text{(A4)}$$

$$\rho_m = \rho(T, S, p_r) \ , \quad \text{(A5)}$$

$$\rho_c = \rho(T_c, S_c, p_r) \ , \quad \text{(A6)}$$

$$\frac{\partial T}{\partial t} + \mathcal{L}T = \mathcal{D}_h T + \frac{\partial}{\partial z}\left(K_h \frac{\partial T}{\partial z}\right) \ , \quad \text{(A7)}$$

$$\frac{\partial S}{\partial t} + \mathcal{L}S = \mathcal{D}_h S + \frac{\partial}{\partial z}\left(K_h \frac{\partial S}{\partial z}\right) \ , \quad \text{(A8)}$$

where u, v, w are the east (λ), north (ϕ) and vertical (z) components of the flow, p is pressure (see below), and ρ_m is the density calculated from the model potential temperature (T) and salinity (S) which, in turn, are updated using the conservation equations defined in Eqs. (A7) and (A8). Here ρ_c is the density calculated from climatological potential temperature (T_c) and salinity (S_c), p_r is the reference pressure at the centre of each z level, K_m and K_h are vertical eddy viscosity and diffusivity coefficients, f is the Coriolis parameter, ρ_o is a reference density, R and g are the Earth's radius and gravitational acceleration, $\mathcal{L}$ is an advection operator defined as:

$$\mathcal{L}q = \frac{1}{R\cos\phi}\frac{\partial (uq)}{\partial \lambda} + \frac{1}{R\cos\phi}\frac{\partial (vq\cos\phi)}{\partial \phi} + \frac{\partial (wq)}{\partial z} \ , \quad \text{(A9)}$$

and $\mathcal{D}_m$ and $\mathcal{D}_h$ are diffusion operators defined as:

$$\mathcal{D}_{(m,h)}q = \frac{1}{R^2}\left\{\frac{1}{\cos^2\phi}\frac{\partial}{\partial \lambda}\left[A_{(m,h)}\frac{\partial q}{\partial \lambda}\right] + \frac{\partial q}{\partial \phi}\left[\cos\phi A_{(m,h)}\frac{\partial q}{\partial \phi}\right]\right\} \ , \quad \text{(A10)}$$

where A_m and A_h are horizontal eddy viscosity and diffusivity coefficients, respectively.

The model uses the subgrid-scale mixing parameterization scheme of Smagorinsky (1963) for the horizontal eddy viscosity A_m and the schemes proposed by Large et al. (1994) for the vertical mixing coefficients K_m and K_h. The turbulent Prandtl Number A_h/A_m is set to 0.1. The model also uses the 4th-order numerics (Dietrich 1997) and Thuburn's flux limiter to discretize the non-linear advection terms in the above equations (Thuburn 1996).

The governing equations presented above are conventional, except for the terms in square brackets on the right side of the hydrostatic equation, Eq. (A4). Here, the conventional density factor in the buoyancy term is replaced by a linear combination of model-computed density ρ_m and climatological density ρ_c: $\alpha\rho_m + (1-\alpha)\rho_c = \rho_m + (1-\alpha)(\rho_c - \rho_m)$, as the main feature of the semiprognostic method suggested by Sheng et al. (2001).

References

Barnier B, Siefridt L, Marchesiello P (1995) Thermal forcing for a global ocean circulation model using a 3-year climatology for ECMWF analyses. J Mar Syst 6: 363–380

da Silva AM, Young CC, Levitus S (1994) Atlas of surface marine data 1994, vol 3. Anomalies of heat and momentum fluxes. NOAA Atlas NESDIS 8, NOAA, Washington, DC, 413 pp

Davidson F, Greatbatch RJ, deYoung B (2001) Asymmetry in the response of a stratified coastal embayment to wind forcing. J Geophys Res 106: 7001–7016

Dengg J, Boening C, Ernst U, Redler R, Beckmann A (1999) Effects of an improved model representation of overflow water on the subpolar North Atlantic. Inter WOCE Newsletter 37: 10–15

Dietrich DE (1997) Application of a modified Arakawa "a" grid ocean model having reduced numerical dispersion to the Gulf of Mexico circulation. Dyn Atmos Oceans 27: 201–217

Dietrich DE, Marietta MG, Roache PJ (1987) An ocean-modelling system with turbulent boundary layers and topography: numerical description. Int J Numer Meth Fluids 7: 833–855

Fox AD, Maskell SJ (1995) Two-way interactive nesting of primitive equation ocean models with topography. J Phys Oceanogr 25: 2977–2996

Fratantoni DF (2001) North Atlantic surface circulation during the 1990s observed with satellite-tracked drifters. J Geophys Res 106: 22067–22093

Ginis I, Richard RA, Rothstein LM (1998) Design of a multiply nested primitive equation ocean model. Mon Weath Rev 126: 1054–1079

Haney RL (1971) Surface thermal boundary conditions for ocean-circulation models. J Phys Oceanogr 1: 241–248

Johns WE, Townsend TL, Fratantoni DM, Wilson WD (2002) On the Atlantic inflow to the Caribbean Sea. Deep-Sea Res I 49: 211–243

Kurihara Y, Tripoli GJ, Bender MA (1979) Design of a movable nested-mesh primitive equation model. Mon Weath Rev 107: 239–249

Large WG, McWilliams JC, Doney SC (1994) Oceanic vertical mixing: a review and a model with a nonlocal boundary layer parameterization. Rev Geophys 32: 363–403

Lu Y, Thompson KR, Wright DG (2001) Tidal currents and mixing in the Gulf of St. Lawrence: an application of the incremental approach to data assimilation. Can J Fish Aquat Sci 58: 723–735

Marchesiello P, WcWilliams JC, Shchepetkin A (2001) Open-boundary conditions for long-term integration of regional oceanic models. Ocean Modelling 3: 1–20

Mooers CNK, Maul GA (1998) Intra-Americas sea circulation, coastal segment(3,W). In: Robinson AR, Brink KH (eds) The sea, vol 11: Wiley, New York, pp 183–208

Murphy SJ, Hurlburt HE, O'Brien JJ (1999) The connectivity of eddy variability in the Caribbean Sea, the Gulf of Mexico, and the Atlantic Ocean. J Geophys Res 104: 1431–1453

Oey L, Chen P (1992) A nested-grid ocean model: with application to the simulation of meanders and eddies in the Norwegian Coastal Current. J Geophys Res 97: 20063–20086

Orlanski I (1976) A simple boundary condition for unbounded hyperbolic flows. J Comput Phys 21: 251–269

Sheinbaum J, Candela J, Badan A, Ochoa J (2002) Flow structure and transport in the Yucatan Channel. Geophys Res Lett 29: 10.1029/2001GL013990

Sheng J (2001) Dynamics of a buoyancy-driven coastal jet: the Gaspé Current. J Phys Oceanogr 31: 3146–3163

Sheng J, Tang L (2003) A numerical study of circulation in the western Caribbean Sea. J Phys Oceanogr 33: 2049–2069

Sheng J, Wright DG, Greatbatch RJ, Dietrich DE (1998) CANDIE: a new version of the DieCAST ocean-circulation model. J Atmos Ocean Tech 15: 1414–1432

Sheng J, Greatbatch RJ, Wright DG (2001) Improving the utility of ocean circulation models through adjustment of the momentum balance. J Geophys Res 106: 16, 711–16, 728

Smagorinsky J (1963) General circulation experiments with the primitive equation, I. The basic experiment. Mon Weath Rev 21: 99–165

Thuburn J (1996) Multidimensional flux-limited advection schemes. J Comput Phys 123: 74–83